Quantum Nonlinear Optics Based on Two-Dimensional Rydberg Atom Arrays

M. Moreno-Cardoner,[1,2] D. Goncalves,[3] and D. E. Chang[3,4]
[1]Institut für Theoretische Physik, Universität Innsbruck, Technikerstrasse 21a, A-6020 Innsbruck, Austria
[2]Departament de Física Quàntica i Astrofísica and Institut de Ciències del Cosmos, Universitat de Barcelona, Martí i Franquès 1, E-08028 Barcelona, Spain
[3]ICFO-Institut de Ciencies Fotoniques, The Barcelona Institute of Science and Technology, 08860 Castelldefels (Barcelona), Spain
[4]ICREA-Institució Catalana de Recerca i Estudis Avançats, 08015 Barcelona, Spain

(Received 14 January 2021; accepted 3 November 2021; published 23 December 2021)

We propose the combination of subwavelength, two-dimensional atomic arrays and Rydberg interactions as a powerful platform to realize strong, coherent interactions between individual photons with high fidelity. The atomic spatial ordering guarantees efficient atom-light interactions without the possibility of scattering light into unwanted directions, allowing the array to act as a perfect mirror for individual photons. In turn, Rydberg interactions enable single photons to alter the optical response of the array within a potentially large blockade radius R_b, which can effectively punch a large "hole" for subsequent photons. We show that such a system enables a coherent photon-photon gate or switch, with a significantly better error scaling ($\sim R_b^{-4}$) than in a disordered ensemble. We also investigate the optical properties of the system in the limit of strong input intensities and show that this many-body quantum driven dissipative system can be modeled well by a semiclassical model based on holes punched in a classical mirror.

DOI: 10.1103/PhysRevLett.127.263602

Introduction.—Rydberg electromagnetically induced transparency (REIT) is a promising approach in the challenging quest to achieve strong coherent interactions between individual photons [1]. In EIT, an additional pump field enables probe photons to hybridize with metastable atomic excitations and propagate without loss [Figs. 1(a) and 1(b)] [2–4]. When the metastable state corresponds to a high-lying Rydberg level (REIT), this effect becomes highly nonlinear as strong atomic Rydberg interactions destroy the EIT transparency condition. Then, a second photon within a "blockade radius" of the first effectively sees a strongly scattering two-level medium, an effect now routinely observed [5–10]. However, despite many spectacular experiments, it remains challenging to functionalize REIT into coherent, single-photon nonlinear devices. A major reason is that the two-level blockaded region is naturally dissipative, scattering photons into random uncontrolled directions. The best known gate protocol has an error that scales with blockade radius (or more properly, optical depth per blockade radius) as $\sim R_b^{-3/2}$ [7].

Rydberg nonlinear optics would be much more robust if an ensemble of two-level atoms could be made completely lossless to resonant light. Remarkably, this occurs when the atoms form a defect-free array with subwavelength lattice constant. Then, the spatial ordering and interference in emission ensure that atoms cannot scatter light into random directions, but only into the same mode (in the backward or forward directions) as the light coming in. The optical properties of arrays have attracted significant interest, especially in the linear optical regime [11–27]. As one particularly relevant example, it has been theoretically predicted [16,18,28] and experimentally observed [22] that a two-dimensional (2D) array can act as a nearly perfect mirror for weak resonant light [Fig. 1(c)]. Nonlinear optics in arrays using the two-level nature of atoms [29–31] or atomic motion [32] are also being explored, as is the conditional linear response based on Rydberg blockade to produce interesting quantum optical states [26,27].

Here, we propose Rydberg interactions in 2D arrays as a powerful platform for quantum nonlinear optics (also recently discussed by Zhang *et al.* [33]). First, we show

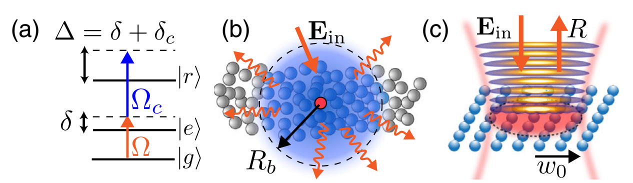

FIG. 1. (a) Level diagram of single three-level atom with ground, excited, and Rydberg levels, and relevant detunings and Rabi frequencies indicated. (b) In REIT in a disordered ensemble, an atom in a Rydberg level (red) creates an effective medium of two-level atoms (blue) within a blockade radius R_b, which strongly scatters near-resonant incident light. (c) An array of two-level atoms (with states $|g, e\rangle$) shown nearly perfectly reflecting a weak resonant Gaussian beam of waist w_0.

how Rydberg dressing interactions lead to strong antibunching in the reflected field, once the blockade radius exceeds the incident beam waist. This inability to simultaneously reflect two photons arises as a reflected photon momentarily punches a large "hole" in the atomic mirror. We then propose a protocol to realize a coherent photon-photon gate or switch, where the presence (absence) of a first photon results in the transmission (reflection) of a second photon, and derive a favorable scaling of gate error as $\sim R_b^{-4}$. Finally, we investigate the response of an array in the limit of high input intensity, where the system exhibits a nontrivial dependence of reflectance, transmittance, and loss on driving power and blockade radius. Although this *a priori* represents a complicated, many-body quantum driven dissipative system, the behavior can be captured well by a semiclassical stochastic model based on holes punched in a mirror.

System and formalism.—We consider a two-dimensional square array (lattice constant d) of $N_a = N^2$ atoms trapped at fixed positions in the $z = 0$ plane. The ground and excited states $|g, e\rangle$ support an optical transition with electric dipole matrix element $\wp$ oriented along one of the lattice axes. Each atom will interact with both an incoming field taken to be a coherent state with spatial mode $\mathbf{E}_{\text{in}}(\mathbf{r})$ and frequency ω_L, and the radiated fields of other atoms. The resulting atomic dynamics are governed by the master equation [34]

$$\dot{\hat{\rho}} = -(i/\hbar)(\mathcal{H}_{\text{eff}}\hat{\rho} - \hat{\rho}\mathcal{H}_{\text{eff}}^{\dagger}) + \sum_{i,j=1}^{N_a} \Gamma^{ij}\hat{\sigma}_j^{ge}\hat{\rho}\hat{\sigma}_i^{eg}, \quad (1a)$$

$$\mathcal{H}_{\text{eff}}/\hbar = -\left(\delta + i\frac{\Gamma_0}{2}\right)\sum_{i=1}^{N_a}\hat{\sigma}_i^{ee} - \sum_{i=1}^{N_a}(\Omega_i\hat{\sigma}_i^{ge} + \text{H.c.}) + \sum_{i,j=1,i\neq j}^{N_a}\left(J^{ij} - i\frac{\Gamma^{ij}}{2}\right)\hat{\sigma}_i^{eg}\hat{\sigma}_j^{ge} + \hat{V}_{\text{Ryd}}. \quad (1b)$$

Here, we define the atomic operators $\hat{\sigma}_i^{\alpha\beta} = |\alpha_i\rangle\langle\beta_i|$ with $\{\alpha, \beta\} \in \{g, e\}$, the detuning $\delta = \omega_L - \omega_0$ with respect to the single-atom bare frequency ω_0, and the Rabi frequency $\Omega_i = \wp \cdot \mathbf{E}_{\text{in}}(\mathbf{r}_i)/\hbar$ of an atom at $\mathbf{r}_i$. We will eventually consider a Gaussian beam focused on the atomic plane, in which case we express $\Omega_i = \Omega_0 e^{-\rho_i^2/w_0^2}$ in terms of a peak Rabi frequency Ω_0, the beam waist w_0, and the in-plane radial coordinate ρ_i. The Rydberg interaction term $\hat{V}_{\text{Ryd}}$ will be specified later. The photon-mediated interactions between atoms are given by

$$J^{ij} - i\Gamma^{ij}/2 = -\frac{\mu_0\omega_0^2}{\hbar}\wp^* \cdot \mathbf{G}(\mathbf{r}_i - \mathbf{r}_j, \omega_0) \cdot \wp, \quad (2)$$

with J^{ij}, $\Gamma^{ij} \in \Re$ describing coherent interactions and collective emission, respectively. $\mathbf{G}(\mathbf{r}, \omega_0)$ is the electromagnetic Green's tensor in free space,

$$\mathbf{G}(\mathbf{r}, \omega_0) = \frac{e^{ik_0 r}}{4\pi k_0^2 r^3}\left[(k_0^2 r^2 + ik_0 r - 1)\mathbb{1} + (-k_0^2 r^2 - 3ik_0 r + 3)\frac{\mathbf{r} \otimes \mathbf{r}}{r^2}\right], \quad (3)$$

with $k_0 = \omega_0/c$. For a single isolated atom, the excited-state spontaneous emission rate is given by $\Gamma^{ii} \equiv \Gamma_0 = \wp^2 k_0^3/(3\pi\hbar\epsilon_0)$.

The atomic dynamics under Eq. (1a) directly encode the emitted field correlations [35–38]. While the atoms emit into all directions, we consider the experimentally realistic scenario where an input mode (e.g., a Gaussian) is defined, and only the light emitted back into the same mode in the backward (reflected) or forward (transmitted) directions is collected. The field operators associated with these detection modes $\mathbf{E}_{\text{det}}(\mathbf{r})$ [with det $= (R, T)$] are [20]

$$\hat{E}_{\text{det}} = \hat{E}_{\text{det,in}} + i\sqrt{\frac{k_0}{2\hbar\epsilon_0 A}}\sum_{j=1}^{N_a}\mathbf{E}_{\text{det}}^*(\mathbf{r}_j) \cdot \wp\hat{\sigma}_j^{ge}, \quad (4)$$

where $\hat{E}_{\text{det,in}}$ is the quantum input field of the particular mode, and $A = \int_{z=\text{const}}\mathbf{E}_{\text{det}}^*(\mathbf{r})\mathbf{E}_{\text{det}}(\mathbf{r})d^2\mathbf{r}$. With this normalization, $\langle\hat{E}_{\text{det}}^{\dagger}\hat{E}_{\text{det}}\rangle$ is the rate of photons emitted in the mode.

The above formalism fully captures the physics of multiple scattering and wave interference of light. As the dynamics depends on the detailed microscopic position configurations, typical quantum theories for disordered ensembles (e.g., to derive gate fidelities [7]) ignore such complicating effects. In contrast, our proposal exploits these effects as a major resource.

Linear regime and perfect reflection.—One important consequence is that an infinite 2D array can behave as a perfect mirror for single photons. Let us consider a plane-wave input field $\sim e^{i\mathbf{k}\cdot\mathbf{r}}$ with in-plane component $\mathbf{k}_{\parallel}$ and normal component satisfying $k_z^2 = (\omega_L/c)^2 - |\mathbf{k}_{\parallel}|^2$. In the linear (single excitation) regime, the driving field only couples to spin waves of the *same* wave vector; for subwavelength lattices ($d < \lambda_0/2 = \pi/k_0$), these spin waves also only reradiate light of wave vector $\mathbf{k}_{\parallel}$ (in the transmitted and reflected directions $\pm k_z$). The reflection and transmission coefficients are [18]

$$r = \frac{\langle\hat{E}_R\rangle}{\langle\hat{E}_{T,\text{in}}\rangle} = -\frac{i\Gamma_{\mathbf{k}_{\parallel}}/2}{\delta - \Delta_{\mathbf{k}_{\parallel}} + i\Gamma_{\mathbf{k}_{\parallel}}/2}, \qquad t = 1 + r. \quad (5)$$

Here, the collective decay rates $\Gamma_{\mathbf{k}_{\parallel}} = (3\pi\Gamma_0/k_0^2 d^2)(1 - |\mathbf{k}_{\parallel}|^2/k_0^2)$ and resonance frequency shifts $\Delta_{\mathbf{k}_{\parallel}} = \sum_{j\neq 0} e^{i\mathbf{k}_{\parallel}\cdot(\mathbf{r}_j - \mathbf{r}_0)}J^{0j}$ of the spin wave mode $\mathbf{k}_{\parallel}$ arise from multiple scattering [39]. Notably, when the driving field resonantly excites a spin wave ($\delta = \Delta_{\mathbf{k}_{\parallel}}$), the array becomes purely reflecting, $|r|^2 = 1$.

Rydberg dressing.—We now add a high-lying Rydberg state $|r\rangle$ coupled to $|e\rangle$ by a uniform classical control field with Rabi frequency Ω_c and detuning δ_c from the bare $|e\rangle$-$|r\rangle$ transition. We also introduce the two-photon detuning $\Delta = \delta + \delta_c$ [Fig. 1(a)]. Rydberg atoms undergo a strong van der Waals interaction, $\hat{V}_{\rm vdW} = \sum_{i<j} C_6 r_{ij}^{-6} \hat{\sigma}_i^{rr} \hat{\sigma}_j^{rr}$, with $r_{ij} = |\mathbf{r}_i - \mathbf{r}_j|$. The presence of a Rydberg excitation and its strong interaction with nearby atoms can alter the optical response of an array within a blockade radius. Indeed, it was previously shown how external control of an ancillary Rydberg atom and subsequent measurements can produce interesting quantum states of light [26]. Here, our goal is to have the Rydberg excitation be generated by incoming photons themselves in order to realize strong, coherent photon-photon interactions. Instead of typical REIT, we consider an alternative Rydberg dressing regime [40,41]. We note that REIT in arrays [33] is highly complementary to our approach; single photons can switch the system from being transmitting to reflecting in REIT, and from reflecting to transmitting in our case. However, as we discuss later, our scheme circumvents an important source of error in the implementation of a single-photon switch.

The dressing operates in the regime $|\delta_c| \gg \Omega_c \gg \Omega_0, |\delta|$. This allows the probe to drive population from $|g\rangle$ to $|e\rangle$ (possibly large for the strong driving regime considered later), while $|e\rangle$-$|r\rangle$ transitions induced by the control field remain virtual and their effect treatable perturbatively. For just a single atom in $|e\rangle$, the control field induces an ac-Stark shift $\Delta_{\rm ac} \approx \Omega_c^2/\delta_c - \Omega_c^4/\delta_c^3$, to order Ω_c^4. We will consider two scenarios in which the dressing is applied. In the first, a probe acts on all atoms beginning in $|g\rangle$, and the dressing interaction modifies the ac-Stark shift for two nearby $|e\rangle$ atoms. In the second, a single Rydberg excitation is first created in a separate photon storage step. The dressing then suppresses the ac-Stark shift for any nearby $|e\rangle$ atom. The effective interaction takes the respective forms $\hat{V}_{\rm Ryd}^{ee} \approx \sum_{i\neq j} V\Theta(R_b - r_{ij}) \hat{\sigma}_i^{ee} \hat{\sigma}_j^{ee}$ or $\hat{V}_{\rm Ryd}^{re} \approx \sum_{i\neq j} V\Theta(R_b - r_{ij}) \hat{\sigma}_i^{ee} \hat{\sigma}_j^{rr}$, where we approximate the spatial dependence by a step function [42]. The strength of V is mainly limited by laser power, while the blockade radius R_b depends on detuning δ_c and the C_6 coefficient. We will largely work in the simplified limit where $V \to \infty$, but discuss corrections as relevant. We also apply the convention that $\Theta(0) = 1$; e.g., nearest neighbors are blockaded when $R_b = d$.

Optical nonlinearities in the weak driving limit.—We now consider a weak resonant ($\Omega_0/\Gamma_0 \to 0$, $\delta = \Delta_{\mathbf{k}_\parallel = 0}$) Gaussian input probe beam with $w_0/d = 0.35N$, so that diffraction from the array edges is negligible, and use Eq. (4) to evaluate the second-order correlation function $g_R^{(2)} = \langle \hat{E}_R^\dagger \hat{E}_R^\dagger \hat{E}_R \hat{E}_R \rangle / \langle \hat{E}_R^\dagger \hat{E}_R \rangle^2$. $g_R^{(2)}$ characterizes the likelihood of immediately detecting a second reflected photon, given detection of a first. Using the dressing interaction $\hat{V}_{\rm Ryd}^{ee}$, we calculate $g_R^{(2)}$ in a two-excitation truncated Hilbert space [42]. Here and in all subsequent calculations, we take $d = \lambda_0/2$.

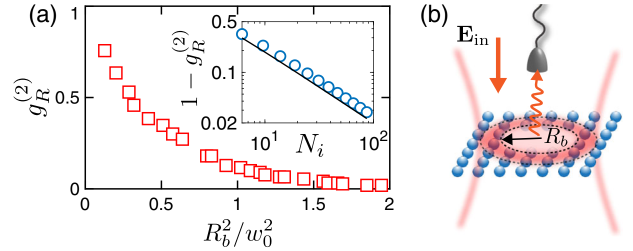

FIG. 2. (a) Second-order correlation function in reflection $g_R^{(2)}$ versus the squared ratio of blockade radius to beam waist $(R_b/w_0)^2$. Inset: $g_R^{(2)}$ without Rydberg interactions versus the approximate number of illuminated atoms $N_i = \pi w_0^2/d^2$ for linear array size $N \in [4, 15]$. The behavior is modeled well by $g_R^{(2)} \sim (1 - 1/N_i)^2$ (solid line). (b) After detecting a first reflected photon, a hole of blockade radius R_b is effectively punched in the atomic mirror.

In Fig. 2(a), we plot $g_R^{(2)}$ versus the squared ratio of blockade radius to beam waist $(R_b/w_0)^2$ for an $N_a = 16^2$ array and $V \to \infty$. $g_R^{(2)}$ is already remarkably reduced from unity when $R_b \sim w_0$, and this "antibunching" becomes perfect ($g_R^{(2)} \to 0$) as R_b increases further. This impossibility of reflecting two photons arises because the first reflected photon must have originated from an excited atom, but $\hat{V}_{\rm Ryd}^{ee}$ prevents the excitation of another nearby atom, effectively punching a hole of radius R_b in the mirror [Fig. 2(b)]. Without Rydberg interactions, the first reflected photon only produces a single-atom hole, such that $g_R^{(2)} \sim (1 - 1/N_i)^2$ [42], where $N_i \sim \pi w_0 0^2/d^2$ is approximately the number of atoms illuminated by the beam [inset of Fig. 2(a)]. Here, $g_R^{(2)} \sim 1$ implies that the first reflected photon has negligible influence on a second photon; i.e., the mirror is highly linear.

These results suggest that a blockaded 2D array is the "ultimate" nonlinear element. It is lossless, unable to scatter light into undesired modes, and allows for 100% efficient atom-light interactions (as evidenced by perfect reflectance), but retains the nonlinearity of an ideal two-level system. We now utilize these concepts to realize a high-fidelity single-photon switch, where instead of responding to weak classical light, the system now explicitly achieves strong interactions between individual photons.

Gate protocol.—We first summarize the main steps of the single-photon switch. Here, the presence (absence) of a first "gate" photon conditions the array to be transmitting (reflecting) for a subsequent "signal" photon. This switch can be directly converted into a photon-photon gate with an additional beam splitter, which converts the propagation direction into a conditional phase. First, the gate pulse, which consists of either zero or one photon, is split and sent

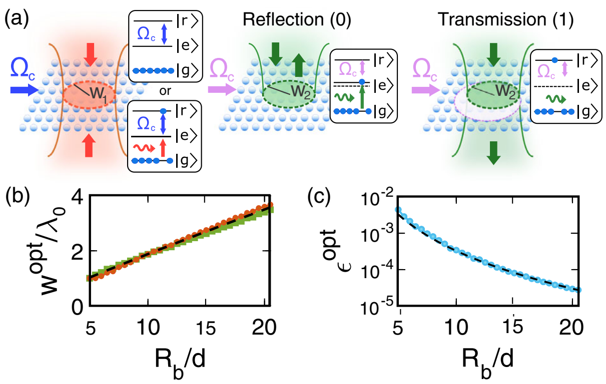

FIG. 3. (a) Schematic of switch protocol. Left panel: a gate pulse (red arrows) consisting of zero (0) or one photon (1) is stored in the Rydberg level via a resonant control field (blue arrow). Afterward, the control field is far detuned to induce Rydberg dressing. A resonant signal photon (green arrows) is then sent from one direction, and depending on the gate photon number is either reflected (0, middle panel) or transmitted (1, right). Transmission occurs as the stored Rydberg excitation punches a hole of radius R_b in the array. The Rydberg excitation and hole center are delocalized over a length $\sim w_1$ corresponding to the gate beam waist, roughly illustrated by the off-center hole in transmission. (b) Optimal beam waists for the gate (red) and signal (green) photons that yield the minimal switch error. The dashed line corresponds to an analytical approximation, Eq. (S.13) in Ref. [42]. (c) Optimal switch error $\epsilon^{\rm opt}$ versus blockade radius R_b/d, along with the analytical approximation Eq. (7) (dashed line).

toward the array from both directions, and stored by applying a resonant control field ($\delta_c \approx -\delta$) to create zero or one Rydberg excitation [Fig. 3(a)]. Afterward, the control field is detuned to implement Rydberg dressing. The signal photon is finally sent from one direction with a frequency adjusted to compensate the single-atom Stark shift induced by the control field. The signal then sees either a perfect resonant mirror or a large transmitting hole, depending on the gate photon number.

We now analyze each step separately. As in other works [7,59], we consider the limit to fidelity arising solely from the finite blockade radius, rather than limited array size. For the storage of the gate pulse, an error of $1-\eta \approx C_s(d)\lambda_0^4/w_1^4$ [20] arises due to its finite beam waist w_1, where $C_s(d)$ is a lattice-constant-dependent coefficient. This equation states that collective behavior of the array reduces if the beam illuminates too few atoms. Sending in the gate pulse from both directions is needed to achieve near-unity efficiency, as the time-reversed process of photon emission [20,60] naturally generates an outgoing photon in both directions. (One-sided illumination would yield a maximum 50% efficiency.)

Now the Rydberg dressing is turned on. Without a gate photon, all atoms are in state $|g\rangle$, and the dressing has no effect. An incoming signal photon with waist w_2 then sees a mirror with a reflectance error due to focusing of $1-R \approx C_R(d)\lambda_0^4/w_2^4$. On the other hand, a gate photon is stored as a delocalized Rydberg excitation $|\Psi\rangle = \sum_i c_i \hat{\sigma}_i^{rg}|g\rangle$, where the state amplitudes follow the Gaussian beam profile $c_i \propto e^{-|\rho_i|^2/w_1^2}$. The Rydberg excitation itself will not interact with the subsequent signal photon on the $|g\rangle$-$|e\rangle$ transition and acts as a single-atom transparent hole. A dressing interaction $\hat{V}^{re}_{\rm Ryd}$ with infinite strength $V \to \infty$ would further extend the radius of the hole to R_b. While here the Rydberg excitation and the blockade radius have the same effect of creating a transparent hole, in REIT, the blockade radius instead would be reflecting [33], while the transparent stored excitation serves as an undesired scattering defect for the signal photon.

As the stored Rydberg excitation is static, the signal photon response is linear optical. Its transmittance T is given by the weighted average [42]

$$T = \frac{\langle \hat{E}_T^\dagger \hat{E}_T \rangle_{\rm sc}}{\langle \hat{E}_{T,\rm in}^\dagger \hat{E}_{T,\rm in} \rangle_{\rm sc}} = \sum_i |c_i|^2 \bar{T}(\mathbf{r}_i, w_2, R_b), \tag{6}$$

where $\bar{T}(\mathbf{r}_i, w_2, R_b)$ is the transmittance of an array with a hole of radius R_b centered on atom i, accounting for the fact that the stored excitation is in a delocalized superposition with weights $|c_i|^2$ [Fig. 3(a)]. Intuitively, efficient transmission requires that the uncertainty of the hole position and the beam waist of the signal photon are small, $w_{1,2} \lesssim R_b$.

Next, we numerically optimize the overall fidelity of the switch. Here, our only approximation involves the modeling of the Rydberg dressing interaction as $\hat{V}^{re}_{\rm Ryd} \approx \sum_{i\neq j} V\Theta(R_b - r_{ij})\hat{\sigma}_i^{ee}\hat{\sigma}_j^{rr}$ with $V \to \infty$, while the storage efficiency η and conditional reflectance and transmittance R, T depending on the gate pulse are evaluated fully numerically [42]. The total switch error ϵ is the maximum error between storage/transmission and reflection, $\epsilon = \max(1-\eta T, 1-R)$. Taking a 41×41 array, we plot the optimal beam waists $w_{1,2}^{\rm opt}$ and minimal errors in Figs. 3(b) and 3(c), respectively, versus R_b. Separately, using a toy model based on the considerations above, we derive an analytical approximation of the error [42]

$$\epsilon^{\rm opt}(R_b, d) \approx C\frac{[1+\log(R_b/d)]^2}{(R_b/d)^4}, \tag{7}$$

which agrees well with full numerics. Notably, the R_b^{-4} scaling significantly outperforms the best gate scaling $\propto R_b^{-3/2}$ in a disordered REIT ensemble [7]. In Ref. [42], we show that this scaling can be realized in realistic settings, accounting for a finite Rydberg interaction strength and realistic potential shape. Finally, although we have taken a large array to isolate the scaling with R_b, we also numerically analyze a small array, which exhibits an additional error due to the beams extending beyond the array. We find that a total error of 1% is already achievable with a 7×7 array.

Strong driving limit.—We now consider the nonlinear resonant ($\delta = \Delta_{\mathbf{k}_\parallel=0}$) response of an array versus arbitrary R_b and coherent state driving power, but within the previously discussed regime of validity of the dressed interaction $\hat{V}^{ee}_{\mathrm{Ryd}}$. We focus on the reflectance and the photon loss $K = 1 - R - T$, the fractional intensity scattered into modes beyond the reflected or transmitted Gaussian fields. We first present numerical results for $N_a = 16$ and $N_a = 36$ square arrays. We directly integrate in time Eq. (1) to find the steady state density matrix (except for the specific case of $N_a = 16$ and $R_b = 0$ where we use an equivalent quantum jump approach [61]). This calculation involves no approximations beyond utilizing an infinite blockade strength $V \to \infty$ to eliminate impossible-to-excite basis states. In Figs. 4(a) and 4(b), we see that the reflectance monotonically decreases with increasing Ω_0 for all blockade radii. This naturally arises from the saturation of the (Rydberg dressed super-) atoms. In contrast, the photon loss varies nonmonotonically

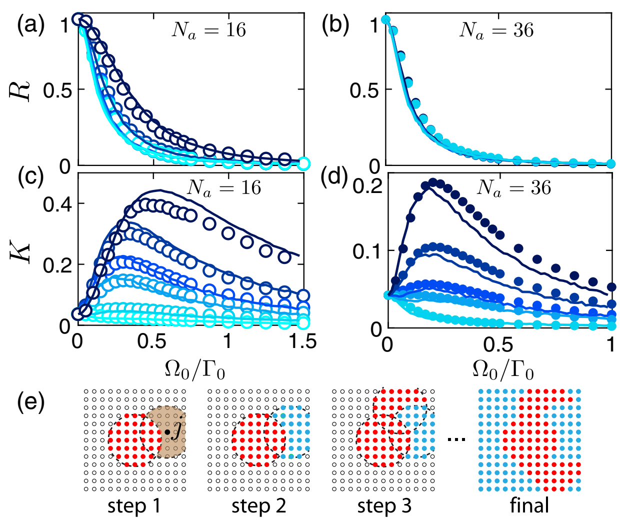

FIG. 4. (a),(b) Reflectance and (c),(d) photon loss versus Rabi frequency Ω_0/Γ_0 for an incident Gaussian beam ($w_0 = 0.4\sqrt{N_a}d$) and an array with $N_a = 16$ or $N_a = 36$. Different colors indicate different blockade radii R_b (from dark to light blue $R_b/d = 0, 1, \sqrt{2}, 2, \sqrt{5}, 3$ for $N_a = 16$ and $R_b/d = \sqrt{8}, \sqrt{10}, 4, \sqrt{18}, 5$ for $N_a = 36$). Symbols denote the exact numerical calculation and solid lines the semiclassical stochastic model. (e) Steps to obtain a configuration used in the model. For each atom j with no assigned state (white circles), a blockade region (brown shaded area in first panel) is defined, comprising all atoms within the blockade radius centered on j except those already assigned a state in a previous step. An unassigned atom among all j is then randomly chosen, and the corresponding blockade region is probabilistically assigned to be reflecting (blue) or saturated (and thus effectively removed, red). The process is iterated until all atoms are assigned (right panel), and the optical properties of this configuration are calculated.

and depends strongly on R_b [Figs. 4(c) and 4(d)]. Furthermore, the maximum loss $K^{\max}$ occurs at some driving strength $|\Omega_0^{\max}|$, with both values depending nontrivially on R_b.

We develop an approximate model of this quantum many-body system in terms of transmitting or diffracting holes punched into a classical mirror [final panel of Fig. 4(e), where red and blue atoms illustrate effectively removed atoms and remaining mirror atoms, respectively]. This assignment proceeds in a series of steps starting with all atoms with no assigned state. Then, regions of radius R_b are randomly selected and assigned to be removed or kept depending on the local probe field intensity, which dictates their probability of saturation [42]. Once all atoms have been assigned [Fig. 4(e)], we calculate the corresponding classical linear loss and reflectance of this particular configuration, repeating and averaging over $\sim$5000 configurations to obtain the loss and reflectance of the system. This semiclassical model captures remarkably well the full system behavior, as the solid lines illustrate in Figs. 4(a)–4(d). If one further assumes that the system roughly consists of N_d independent and nonoverlapping blockade regions, which each have radius R_b and see equal Rabi frequencies Ω, and neglects corrections associated with finite array size, this model predicts a maximum loss of $K^{\max} = (1 - N_d^{-1})/2$ [42]. In particular, the loss vanishes when the system is fully blockaded and allows only a single excitation ($N_d = 1$).

Conclusions and outlook.—2D atomic arrays with Rydberg interactions constitute a powerful platform for quantum nonlinear optics and enable a gate with an error scaling better than that of a disordered ensemble. This work should stimulate immediate possibilities for experiments, such as in quantum gas microscope setups, where efficient reflectance [22] and Rydberg dressing [40,41] have already been separately demonstrated. Although we have focused on 2D arrays here, we anticipate that studying quantum nonlinear optics in arrays more broadly will be a rich area of research, giving rise to other enhanced protocols and novel phenomenology.

The authors acknowledge stimulating discussions with I. Bloch, L. Tarruell, and F. Andreoli. D. E. C. acknowledges support from the European Union's Horizon 2020 research and innovation programme, under European Research Council grant agreement No. 101002107 (NEWSPIN) and FET-Open grant agreement No. 899275 (DAALI), the Government of Spain (Europa Excelencia program Grant No. EUR2020-112155, Severo Ochoa Grant No. CEX2019-000910-S [MCIN/AEI/10.13039/501100011033], and MCIN Plan Nacional Grant PGC2018-096844-B-I00), Generalitat de Catalunya through the CERCA program, Fundació Privada Cellex, Fundació Mir-Puig, Fundación Ramón Areces Project CODEC, and Secretaria d'Universitats i Recerca del Departament d'Empresa i Coneixement de la Generalitat de Catalunya, co-funded by the European Union Regional Development Fund within the ERDF Operational Program of Catalunya (project QuantumCat, ref. 001-P-001644). D. G. aknowledges support from the Secretaria d'Universitats i Recerca de la Generalitat de Catalunya and the European Social Fund (Grant No. 2020 FI B 00196). M. M. C. acknowledges support from the European Union's Horizon 2020 research and innovation program under the Marie Skłodowska-Curie Grant agreement No. 801110, the Government of Spain (Grant No. PID2020-114626GB-I00 from the MICIN/AEI/ 10.13039/501100011033), and the Austrian Federal Ministry of Education, Science and Research (BMBWF). It reflects only the author's view and the Agency is not responsible for any use that may be made of the information it contains.

M. M.-C. and D. G. contributed equally to this work.

[1] D. E. Chang, V. Vuletić, and M. D. Lukin, Quantum nonlinear optics — photon by photon, Nat. Photonics **8**, 685 (2014).

[2] M. Fleischhauer, A. Imamoglu, and J. P. Marangos, Electromagnetically induced transparency: Optics in coherent media, Rev. Mod. Phys. **77**, 633 (2005).

[3] D. F. Phillips, A. Fleischhauer, A. Mair, R. L. Walsworth, and M. D. Lukin, Storage of Light in Atomic Vapor, Phys. Rev. Lett. **86**, 783 (2001).

[4] C. Liu, Z. Dutton, C. H. Behroozi, and L. V. Hau, Observation of coherent optical information storage in an atomic medium using halted light pulses, Nature (London) **409**, 490 (2001).

[5] O. Firstenberg, T. Peyronel, Q.-Y. Liang, A. V. Gorshkov, M. D. Lukin, and V. Vuletić, Attractive photons in a quantum nonlinear medium, Nature (London) **502**, 71 (2013).

[6] S. Baur, D. Tiarks, G. Rempe, and S. Dürr, Single-Photon Switch Based on Rydberg Blockade, Phys. Rev. Lett. **112**, 073901 (2014).

[7] J. D. Thompson, T. L. Nicholson, Q.-Y. Liang, S. H. Cantu, A. V. Venkatramani, S. Choi, I. A. Fedorov, D. Viscor, T. Pohl, M. D. Lukin, and V. Vuleti, Symmetry-protected collisions between strongly interacting photons, Nature (London) **542**, 206 (2017).

[8] D. Tiarks, S. Schmidt-Eberle, T. Stolz, G. Rempe, and S. Dürr, A photon–photon quantum gate based on Rydberg interactions, Nat. Phys. **15**, 124 (2019).

[9] J. D. Pritchard, D. Maxwell, A. Gauguet, K. J. Weatherill, M. P. A. Jones, and C. S. Adams, Cooperative Atom-Light Interaction in a Blockaded Rydberg Ensemble, Phys. Rev. Lett. **105**, 193603 (2010).

[10] H. Gorniaczyk, C. Tresp, J. Schmidt, H. Fedder, and S. Hofferberth, Single-Photon Transistor Mediated by Interstate Rydberg Interactions, Phys. Rev. Lett. **113**, 053601 (2014).

[11] H. Zoubi and H. Ritsch, Lifetime and emission characteristics of collective electronic excitations in two-dimensional optical lattices, Phys. Rev. A **83**, 063831 (2011).

[12] S. D. Jenkins and J. Ruostekoski, Controlled manipulation of light by cooperative response of atoms in an optical lattice, Phys. Rev. A **86**, 031602 (2012).

[13] D. Plankensteiner, L. Ostermann, H. Ritsch, and C. Genes, Selective protected state preparation of coupled dissipative quantum emitters, Sci. Rep. **5**, 16231 (2015).

[14] R. J. Bettles, S. A. Gardiner, and C. S. Adams, Cooperative ordering in lattices of interacting two-level dipoles, Phys. Rev. A **92**, 063822 (2015).

[15] R. J. Bettles, S. A. Gardiner, and C. S. Adams, Cooperative eigenmodes and scattering in one-dimensional atomic arrays, Phys. Rev. A **94**, 043844 (2016).

[16] R. J. Bettles, S. A. Gardiner, and C. S. Adams, Enhanced Optical Cross Section via Collective Coupling of Atomic Dipoles in a 2D Array, Phys. Rev. Lett. **116**, 103602 (2016).

[17] R. T. Sutherland and F. Robicheaux, Collective dipole-dipole interactions in an atomic array, Phys. Rev. A **94**, 013847 (2016).

[18] E. Shahmoon, D. S. Wild, M. D. Lukin, and S. F. Yelin, Cooperative Resonances in Light Scattering from Two-Dimensional Atomic Arrays, Phys. Rev. Lett. **118**, 113601 (2017).

[19] J. Perczel, J. Borregaard, D. E. Chang, H. Pichler, S. F. Yelin, P. Zoller, and M. D. Lukin, Topological Quantum Optics in Two-Dimensional Atomic Arrays, Phys. Rev. Lett. **119**, 023603 (2017).

[20] M. T. Manzoni, M. Moreno-Cardoner, A. Asenjo-Garcia, J. V. Porto, A. V. Gorshkov, and D. E. Chang, Optimization of photon storage fidelity in ordered atomic arrays, New J. Phys. **20**, 083048 (2018).

[21] A. Piñeiro Orioli and A. M. Rey, Dark States of Multilevel Fermionic Atoms in Doubly Filled Optical Lattices, Phys. Rev. Lett. **123**, 223601 (2019).

[22] J. Rui, D. Wei, A. Rubio-Abadal, S. Hollerith, J. Zeiher, D. M. Stamper-Kurn, C. Gross, and I. Bloch, A subradiant optical mirror formed by a single structured atomic layer, Nature (London) **583**, 369 (2020).

[23] Y. X. Zhang and K. Mølmer, Theory of Subradiant States of a One-Dimensional Two-Level Atom Chain, Phys. Rev. Lett. **122**, 203605 (2019).

[24] Y.-X. Zhang, C. Yu, and K. Mølmer, Subradiant bound dimer excited states of emitter chains coupled to a one dimensional waveguide, Phys. Rev. Research **2**, 013173 (2020).

[25] A. Piñeiro Orioli and A. M. Rey, Subradiance of multilevel fermionic atoms in arrays with filling $n \geq 2$, Phys. Rev. A **101**, 043816 (2020).

[26] R. Bekenstein, I. Pikovski, H. Pichler, E. Shahmoon, S. F. Yelin, and M. D. Lukin, Quantum metasurfaces with atom arrays, Nat. Phys. **16**, 676 (2020).

[27] Z.-Y. Wei, D. Malz, A. González-Tudela, and J. I. Cirac, Generation of photonic matrix product states with Rydberg atomic arrays, Phys. Rev. Research **3**, 023021 (2021).

[28] F. Garcia de Abajo, Colloquium: Light scattering by particle and hole arrays, Rev. Mod. Phys. **79**, 1267 (2007).

[29] R. J. Bettles, M. D. Lee, S. A. Gardiner, and J. Ruostekoski, Quantum and nonlinear effects in light transmitted through planar atomic arrays, Communications in Physics **3**, 141 (2020).

[30] A. Cidrim, T. S. do Espirito Santo, J. Schachenmayer, R. Kaiser, and R. Bachelard, Photon Blockade with Ground-State Neutral Atoms, Phys. Rev. Lett. **125**, 073601 (2020).

[31] L. A. Williamson, M. O. Borgh, and J. Ruostekoski, Superatom Picture of Collective Nonclassical Light Emission and Dipole Blockade in Atom Arrays, Phys. Rev. Lett. **125**, 073602 (2020).

[32] E. Shahmoon, M. D. Lukin, and S. F. Yelin, Quantum optomechanics of a two-dimensional atomic array, Phys. Rev. A **101**, 063833 (2020).

[33] L. Zhang, V. Walther, K. Mølmer, and T. Pohl, Photon-photon interactions in Rydberg-atom arrays, arXiv:2101.11375.

[34] P. Meystre and M. Sargent, *Elements of Quantum Optics* (Springer-Verlag, Berlin, 2007).

[35] T. Gruner and D.-G. Welsch, Green-function approach to the radiation-field quantization for homogeneous and inhomogeneous Kramers-Kronig dielectrics, Phys. Rev. A **53**, 1818 (1996).

[36] H. T. Dung, L. Knöll, and D.-G. Welsch, Resonant dipole-dipole interaction in the presence of dispersing and absorbing surroundings, Phys. Rev. A **66**, 063810 (2002).

[37] S. Y. Buhmann and D.-G. Welsch, Dispersion forces in macroscopic quantum electrodynamics, Prog. Quantum Electron. **31**, 51 (2007).

[38] A. Asenjo-Garcia, J. D. Hood, D. E. Chang, and H. J. Kimble, Atom-light interactions in quasi-one-dimensional nanostructures: A Green's-function perspective, Phys. Rev. A **95**, 033818 (2017).

[39] A. Asenjo-Garcia, M. Moreno-Cardoner, A. Albrecht, H. J. Kimble, and D. E. Chang, Exponential Improvement in Photon Storage Fidelities Using Subradiance and "Selective Radiance" in Atomic Arrays, Phys. Rev. X **7**, 031024 (2017).

[40] J. Zeiher, R. van Bijnen, P. Schauß, S. Hild, J.-y. Choi, T. Pohl, I. Bloch, and C. Gross, Many-body interferometry of a Rydberg-dressed spin lattice, Nat. Phys. **12**, 1095 (2016).

[41] J. Zeiher, J.-y. Choi, A. Rubio-Abadal, T. Pohl, R. van Bijnen, I. Bloch, and C. Gross, Coherent Many-Body Spin Dynamics in a Long-Range Interacting Ising Chain, Phys. Rev. X **7**, 041063 (2017).

[42] See Supplemental Material at http://link.aps.org/supplemental/10.1103/PhysRevLett.127.263602 for more details on the Rydberg dressing potential, the low driving intensity limit, the single-photon switch and the strong driving limit, which includes Refs. [43–58].

[43] N. Henkel, R. Nath, and T. Pohl, Three-Dimensional Roton Excitations and Supersolid Formation in Rydberg-Excited Bose-Einstein Condensates, Phys. Rev. Lett. **104**, 195302 (2010).

[44] T. Macrì and T. Pohl, Rydberg dressing of atoms in optical lattices, Phys. Rev. A **89**, 011402(R) (2014).

[45] P. Kościk and T. Sowiński, Exactly solvable model of two interacting Rydberg-dressed atoms confined in a two-dimensional harmonic trap, Sci. Rep. **9**, 12018 (2019).

[46] S. Bravyi, D. DiVincenzo, and D. Loss, Schrieffer–Wolff transformation for quantum many-body systems, Ann. Phys. (Amsterdam) **326**, 2793 (2011).

[47] T. Peyronel, O. Firstenberg, Q.-Y. Liang, S. Hofferberth, A. V. Gorshkov, T. Pohl, M. D. Lukin, and V. Vuletić, Quantum nonlinear optics with single photons enabled by strongly interacting atoms, Nature (London) **488**, 57 (2012).

[48] E. Distante, P. Farrera, A. Padrón-Brito, D. Paredes-Barato, G. Heinze, and H. de Riedmatten, Storing single photons emitted by a quantum memory on a highly excited Rydberg state, Nat. Commun. **8**, 14072 (2017).

[49] I. I. Ryabtsev, I. I. Beterov, D. B. Tret'yakov, V. M. Èntin, and E. A. Yakshina, Spectroscopy of cold rubidium Rydberg atoms for applications in quantum information, Phys. Usp. **59**, 196 (2016).

[50] D. Steck, Rubidium 87D line data, available online at http://steck.us/alkalidata (2010).

[51] A. Asenjo-Garcia, H. J. Kimble, and D. E. Chang, Optical waveguiding by atomic entanglement in multilevel atom arrays, Proc. Natl. Acad. Sci. U.S.A. **116**, 25503 (2019).

[52] J. B. Balewski, A. T. Krupp, A. Gaj, S. Hofferberth, R. Löw, and T. Pfau, Rydberg dressing: understanding of collective many-body effects and implications for experiments, New J. Phys. **16**, 063012 (2014).

[53] A. Browaeys, D. Barredo, and T. Lahaye, Experimental investigations of dipole–dipole interactions between a few Rydberg atoms, J. Phys. B **49**, 152001 (2016).

[54] L. Béguin, A. Vernier, R. Chicireanu, T. Lahaye, and A. Browaeys, Direct Measurement of the van der Waals Interaction between Two Rydberg Atoms, Phys. Rev. Lett. **110**, 263201 (2013).

[55] R. Löw, H. Weimer, J. Nipper, J. B. Balewski, B. Butscher, H. P. Büchler, and T. Pfau, An experimental and theoretical guide to strongly interacting Rydberg gases, J. Phys. B **45**, 113001 (2012).

[56] S. Hollerith, J. Zeiher, J. Rui, A. Rubio-Abadal, V. Walther, T. Pohl, D. M. Stamper-Kurn, I. Bloch, and C. Gross, Quantum gas microscopy of Rydberg macrodimers, Science **364**, 664 (2019).

[57] T. Shi, D. E. Chang, and J. I. Cirac, Multiphoton-scattering theory and generalized master equations, Phys. Rev. A **92**, 053834 (2015).

[58] K. Tanaka, N. Saga, and H. Mizokami, Field spread of a diffracted Gaussian beam through a circular aperture, Appl. Opt. **24**, 1102 (1985).

[59] A. V. Gorshkov, J. Otterbach, M. Fleischhauer, T. Pohl, and M. D. Lukin, Photon-Photon Interactions via Rydberg Blockade, Phys. Rev. Lett. **107**, 133602 (2011).

[60] A. V. Gorshkov, A. André, M. Fleischhauer, A. S. Sørensen, and M. D. Lukin, Universal Approach to Optimal Photon Storage in Atomic Media, Phys. Rev. Lett. **98**, 123601 (2007).

[61] H. Carmichael, *An Open Systems Approach to Quantum Optics* (Springer, Berlin, 1991).